

The relevance of continuous variable entanglement in DNA

Elisabeth Rieper^{1*}, Janet Anders^{2†} and Vlatko Vedral^{1,3,4}

¹Center for Quantum Technologies, National University of Singapore, Republic of Singapore;

²Department of Physics and Astronomy, University College London, London WC1E 6BT, United Kingdom;

³Atomic and Laser Physics, Clarendon Laboratory,

University of Oxford, Parks Road, Oxford OX13PU, United Kingdom

⁴Department of Physics, National University of Singapore, Republic of Singapore.

(Dated: June 23, 2013)

SUMMARY We consider a chain of harmonic oscillators with dipole-dipole interaction between nearest neighbours resulting in a van der Waals type bonding. The binding energies between entangled and classically correlated states are compared. We apply our model to DNA. By comparing our model with numerical simulations [1] we conclude that entanglement may play a crucial role in explaining the stability of the DNA double helix.

PACS numbers:

Introduction.— The growing field of quantum biology deals with the question if living systems use non-trivial quantum effects to optimise some tasks. Studies range from the role of quantum physics in photosynthesis [2–5] and in the avian compass [6, 7], through to the observation that ‘warm and wet’ living systems can embody entanglement given a suitable cyclic driving [8]. Except for [9], where the possibility of intramolecular refrigeration is discussed, all the above works focus on spin entanglement. In this Letter we raise the question about the importance of continuous variable (CV) entanglement [21] in macromolecules like DNA. We look at continuously interacting subsystems of the DNA strand. This is not to be confused with a full chemical bonding, where electrons are shared between atoms. Also the question of existence of entanglement is non trivial, as for weak interaction or high temperature the state of the system might still be separable.

Our work was motivated by a numerical study on the importance of dispersion energies in DNA [1]. Dispersion energies describe attractive van der Waals forces between non-permanent dipoles. Recently many works [10, 11] realised its importance to stabilise macromolecules. Modelling macromolecules like DNA faces the problem of the huge number of atoms. This makes it nearly impossible to fully quantum mechanically simulate the system. Therefore several techniques have been invented in quantum chemistry to simulated with simplified dynamics. In [1] the authors first quantum mechanically optimise a small fragment of DNA in the water environment. Second, they performed various molecular dynamics (MD) simulations in explicit water based either fully on the empirical potential or on more accurate QM/ MM MD simulations. The molecular dynamics simulations were performed with an AMBER parm9916 empirical force

field and the following modifications were introduced in the non-bonded part, which describes the potential energy of the system (see eq 1) and is divided into the electrostatic and Lennard-Jones terms. The former term is modelled by the Coulomb interaction of atomic point-charges, whereas the latter describes repulsion and dispersion energies.’

$$V(r) = \frac{q_i q_j}{4\pi\epsilon_0 r_{ij}} + 4\epsilon \left[\left(\frac{\sigma}{r_{ij}} \right)^{12} - \left(\frac{\sigma}{r_{ij}} \right)^6 \right] \quad (1)$$

Modifications of the dispersion energy were introduced by scaling the parameter ϵ . For $\epsilon = 1$ the dynamics of the DNA strand is normal. For $\epsilon = 0.01$ there is an increase of 27% in energy in the DNA. This causes the DNA to unravel from the double helix form to a ladder, which cannot fulfil its biological function.

Here we want to investigate with a simple model of DNA whether CV entanglement can be present at room temperature DNA, and if this entanglement is connected to the energy of the molecule. We are aware that there are many technically more advanced quantum chemically calculations for van der Waals type interaction, i.e. [12]. The aim of this work is not to provide the most accurate model (which is due to the complexity of DNA very difficult anyway), but to give a model that allows to understand the basic principle of non-local interaction.

The Model.— We develop a simple model that allows us to understand the basic features of energy reduction in large molecules. The nucleic bases adenine, guanine, cytosine and thymine are planar molecules surrounded by π electron clouds. We model each pair of adenine-thymine and guanine-cytosine as an immobile positively charged centre and the outer electron cloud free to move around its equilibrium position, see fig. 1. As the charges balance, there is no permanent dipole moment. When the centre of the negative charges does not coincide with the positive centre, there is however a non-permanent dipole

*elisabeth.rieper@quantumlah.org

†janet@qipc.org

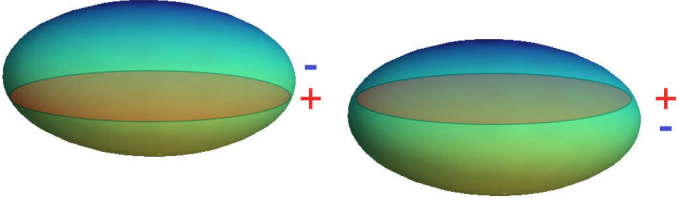


FIG. 1: This graphic shows a sketch of a DNA nucleic acid base pair. The mostly planar molecules are divided into the positively charged molecule core (red) and the negatively charged outer π electron cloud (blue-yellow). In equilibrium the centre of both parts coincide, thus there is no permanent dipole. If the electron cloud oscillates around the core, a non permanent dipole is created [17]. The deviation out of equilibrium is denoted by (x, y, z) . The corresponding dipole is $\vec{\mu} = Q(x, y, z)$. This oscillation might be caused by an external field, or via van der Waals interaction with another non permanent dipole, as it is given in a DNA strand.

moment. We denote the displacement of the two centres by (x, y, z) . We also assume the deviation out of equilibrium $|(x, y, z)|$ to be small compared to the distance r between nearest neighbours in chain. Each base pair is described by a harmonic oscillator with trapping potential Ω . The DNA strand is treated like a chain of harmonic oscillators, see fig. 2. Two neighbouring base pairs at distance r have dipole-dipole interaction.

In the following we will use the Hamiltonian

$$H = \sum_{j,d=x,y,z}^N \left(\frac{p_{j,d}^2}{2m} + \frac{m\Omega_d^2}{2} d_j^2 + V_{dip-dip} \right) \quad (2)$$

where d denotes the dimensional degree of freedom, and the dipole potential

$$V_{dip-dip} = \sqrt{\epsilon} \frac{1}{4\pi\epsilon_0 r^3} (3(\vec{\mu}_j \vec{r}_N)(\vec{\mu}_{j+1} \vec{r}_N) - \vec{\mu}_j \vec{\mu}_{j+1}) \quad (3)$$

with $\vec{\mu}_j = Q(x, y, z)$ dipole vector of of site j and \vec{r}_N normalised distance vector between site j and $j+1$. Due to symmetry \vec{r}_N is independent of j . The dimensionless scaling factor ϵ has a identical role like in [1]. In order to compare our model with [1], we will look at normal interaction $\epsilon = 1$ and scaled interaction $\epsilon = 0.01$. The distance between neighbouring sites in DNA is usually around $r_0 = 4.5\text{\AA}$. For generality we will not fix the distance.

Due to the double helix form the dipole potential has coupling terms of the form xz etc. Detailed analysis following [13] shows that the energy contribution from the cross coupling terms is small, hence they will be ignored here. This leads to the interaction term

$$V_{dip-dip} = \sqrt{\epsilon} \frac{Q^2}{4\pi\epsilon_0 r^3} (-x_j x_{j+1} - y_j y_{j+1} + 2z_j z_{j+1}) \quad (4)$$

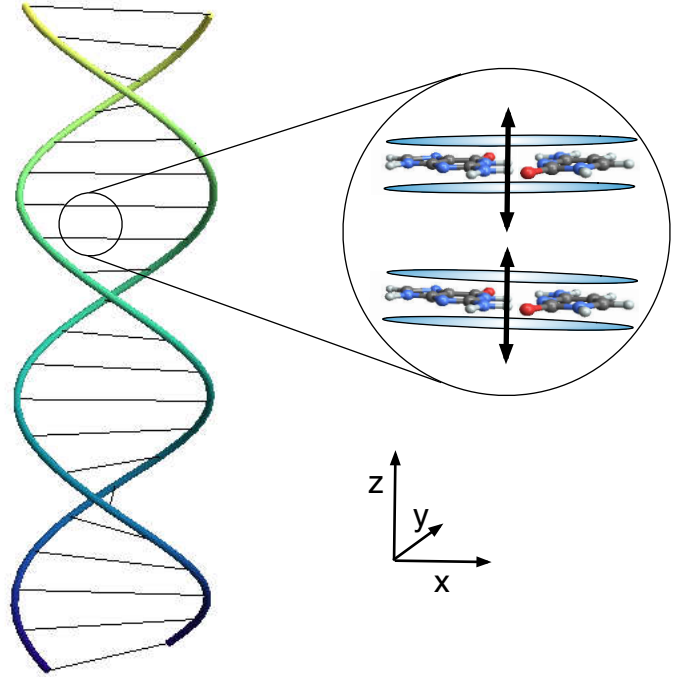


FIG. 2: This graphic shows a sketch of a DNA strand. The chain is along z direction. Each bar in the double helix represents one DNA base pair, either adenine-thymine (AT) or guanine-cytosine (GC). The inset shows two simplified GC base pairs. Around the core of atoms is the blue outer electron cloud. The oscillation of these electron clouds is modelled here as non-permanent harmonic dipoles, which are depicted by the black arrows.

The different signs for x, y and z reflect the orientation of the chain along z direction.

A discrete Fourier transformation of the form

$$d_j = \frac{1}{\sqrt{N}} \sum_{l=1}^N e^{i\frac{2\pi}{N}jl} \tilde{d}_l$$

$$p_{j,d} = \frac{1}{\sqrt{N}} \sum_{l=1}^N e^{-i\frac{2\pi}{N}jl} \tilde{p}_{l,d} \quad (5)$$

decouples the system into independent phonon modes. These modes can be diagonalized by introducing creation $a_{d,l} = \sqrt{\frac{m\Omega_d}{2\hbar}} \left(\tilde{d} + \frac{i}{m\Omega_d} \tilde{p}_{l,d} \right)$ and annihilation operator $a_{d,l}^\dagger$. This results in the dispersion relations

$$\omega_{xl}^2 = \Omega_x^2 + 2 \left(2 \sin^2 \left(\frac{\pi l}{N} \right) - 1 \right) \frac{\sqrt{\epsilon} Q^2}{4\pi\epsilon_0 r^3 m} \quad (6)$$

$$\omega_{yl}^2 = \Omega_y^2 + 2 \left(2 \sin^2 \left(\frac{\pi l}{N} \right) - 1 \right) \frac{\sqrt{\epsilon} Q^2}{4\pi\epsilon_0 r^3 m} \quad (7)$$

$$\omega_{zl}^2 = \Omega_z^2 + 4 \left(2 \cos^2 \left(\frac{\pi l}{N} \right) - 1 \right) \frac{\sqrt{\epsilon} Q^2}{4\pi\epsilon_0 r^3 m} \quad (8)$$

and the Hamiltonian in diagonal form

$$H = \sum_{l=1, d=x,y,z}^N \left(\hbar\omega_{dl} \left(n_{d,l} + \frac{1}{2} \right) \right), \quad (9)$$

where $n_{d,l} = a_{d,l}^\dagger a_{d,l}$ is the number operator of mode l in direction d . The trapping potentials Ω_d can be linked to experimental data (see table I) through the relation $\Omega_d = \sqrt{\frac{Q^2}{m_e \alpha_d}}$, where α_d is the polarizability of the nucleid base. Although the values for the four bases differ,

TABLE I: Numerical values for polarizability of different nucleid acid bases [18] in units of $1au = 0.164 \cdot 10^{-40} Fm^2$. The trapping frequencies are calculated using the formula $\Omega = \sqrt{\frac{Q^2}{m_e \alpha}}$ and are given in units of $10^{15} \frac{1}{s}$.

nucleid acid	α_x	α_y	α_z	Ω_x	Ω_y	Ω_z
adenine	102.5	114.0	49.6	4.1	3.9	6.0
cytosine	78.8	107.1	44.2	4.7	4.1	6.3
guanine	108.7	124.8	51.2	4.0	3.8	5.9
thymine	80.7	101.7	45.9	4.7	4.2	6.2

all of them show roughly twice as large polarizabilities in x, y direction, i.e. transverse to the direction of the chain. In the following we will approximate the chain to have the same value of trapping potential at each site. In x, y direction we will use $\Omega_{x,y} = 4 \cdot 10^{15} \frac{1}{s}$, and in z direction $\Omega_z = 6 \cdot 10^{15} \frac{1}{s}$. Here we assumed the number of involved electrons to be one. Although the value of Ω_d changes for more electrons, both the entanglement and the energy ratio of entangled over separable state stays invariant. As the involved frequencies are in the optical range, the system is effectively in the ground state.

Entanglement and Energy.-

Clearly the chain of coupled harmonic oscillator is entangled at zero temperature, but is it possible to have entanglement at room temperature? There is an easy to calculate criterion for nearest neighbour entanglement for harmonic chains [14], which compares the temperature with the coupling strength between neighbouring sites. In general, for $\frac{2k_B T}{\hbar\omega} < 1$ one can expect entanglement to exist. Here the coupling strength is given by $\omega = \sqrt{\epsilon \frac{Q^2}{4\pi\epsilon_0 m r^3}} \approx 1.6 \cdot 10^{15} \frac{1}{s}$ for $r = 4.5 \text{ \AA}$, which leads to $\frac{2k_B 300K}{\hbar\omega} = 0.05$ for $\epsilon = 1$ and 0.16 for $\epsilon = 0.01$. The coupling is dominant compared to the temperature, which explains the existence of room temperature entanglement. In the next step we are going to quantify the amount of entanglement. For Gaussian states there is an easy to compute entanglement criteria, namely the positivity of the reduced covarianz matrix of a state [15].

$$0 \leq S_{1,2} = \frac{1}{\hbar^2} \langle (d_j \pm d_{j+1})^2 \rangle \langle (p_{d,j} \mp p_{d,j+1})^2 \rangle - 1 \quad (10)$$

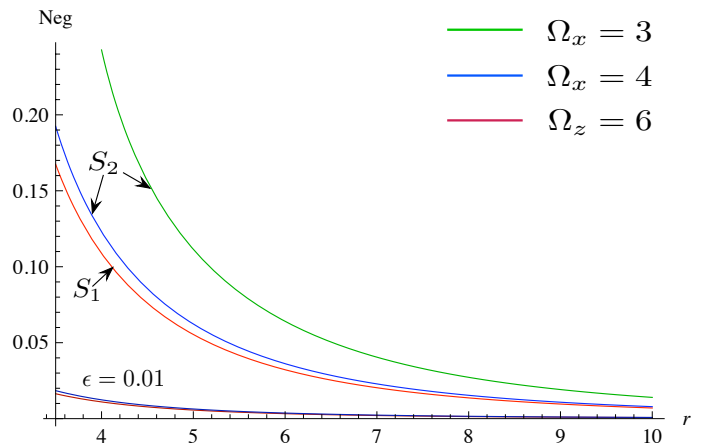


FIG. 3: This graphic shows the nearest neighbour negativity as a function of distance between sites in \AA at $T = 300K$. The three upper curves are for scaling factor $\epsilon = 1$, the lower two curves are for scaling factor $\epsilon = 0.01$. The red curve is for z direction and $\Omega_z = 6 \cdot 10^{15} \frac{1}{s}$. The blue and green curve are for x direction and $\Omega_x = 4 \cdot 10^{15} \frac{1}{s}$ and $\Omega_x = 3 \cdot 10^{15} \frac{1}{s}$. The lower value of trapping potential has a higher value of negativity, but the chain also becomes unstable for small values of r . The negativity for $\epsilon = 0.01$ is much smaller than in the unscaled case. This has consequences for the energy saving, see Fig. 4.

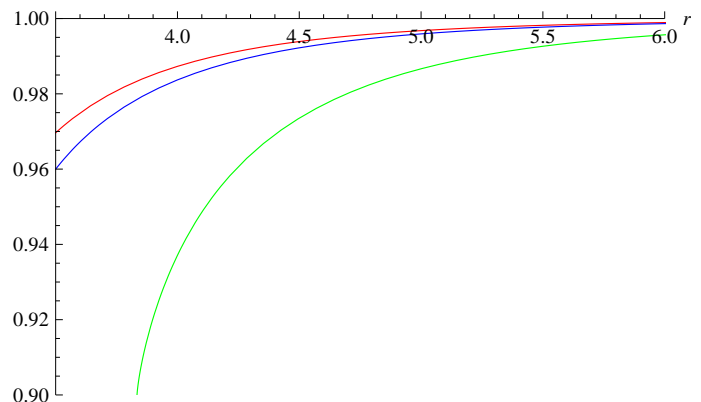


FIG. 4: This graphic shows the ratio of energy of entangled state over separable thermal state dependant on the nearest neighbour distance r in \AA . The same colour coding like in Fig. 3 applies. All curves are for $\epsilon = 1$.

with d_j position operator of site j in direction d and $p_{d,j}$ corresponding momentum operator. If the inequality is violated, the sites j and $j+1$ are entangled. The negativity, a widely used measure for entanglement, is calculated using the formula $N = \sum_{k=1}^2 \max[0, -\ln \sqrt{S_k + 1}]$. The results are shown in Fig. 3.

The amount of negativity strongly depends on the distance r between sites and the value of trapping potential Ω . The lower the potential, the higher the negativity. For the scaled interaction the chain is still en-

tangled, but the amount of negativity can be neglected. Interestingly, along the chain the S_1 criterion is violated, whereas transversal to the chain S_2 is violated. This reflects the geometry of the chain. Along the main axes of the chain energy is reduced by correlated movement. Transversal to the chain it is energetically better to be anti-correlated.

Now we are going to compare the energy per site of an entangled state with a separable one. As the effective temperature is very low for the chain, we restrict our analysis to the ground state. The energy of the ground state for the degree of freedom $d = x, y, z$ is given by $E_{d,ent} = \langle H_d \rangle = \sum_{l=1}^N \frac{\hbar \omega_{dl}}{2N}$. For a separable state of the system expectation values take the form $\langle d_j d_{j+1} \rangle = \langle d_j \rangle \langle d_{j+1} \rangle$. For a thermal state the lower bound of this expectation value is zero. This is equivalent to identical dispersion relation for each phonon mode (or, similarly, the loss of dispersion energy). Hence the energy per site for a thermal separable state is just given by $E_{d,sep} = \frac{\hbar \Omega_d}{2}$. Fig. 4 shows the ratio of energy of entangled over separable states, $\frac{E_{d,ent}}{E_{d,sep}}$. For $r = 4.5\text{\AA}$ the energy reduction is around 1% in both x, y and z direction. This clearly does not fully account for the reported energy increase of 27% per base pair. One shortcoming of this simple model is that it rather describes a single strand of DNA, which means that only 13.5% energy increase are to be expected. Fig. 4 also shows that the exact amount of energy reduction compared to the separable state is very sensitive to the value of the trapping potential Ω . In case the real potentials vary slightly from the values we used, the energy will also change.

Comparison with non-thermal correlations.— The above considerations compare the energy of an entangled state with a separable thermal state. If the separable state is not thermal, conclusions might change [16]. Here we want to investigate one class of models having classical correlations. We include a local driving force F_j to each site j to the Hamiltonian. This driving will induce a dipole at each site. We restrict ourselves to the x direction, but similar arguments also hold in y and z dimension. In the first step we solve the dynamics for a single harmonic oscillator with driving and look at the energy increase due to driving. In the second step we compare this local energy change with the interaction energy of two neighbouring sites.

The effective local Hamiltonian looks like

$$H_{j,eff} = \frac{p_{j,x}^2}{2m} + \frac{m\Omega_x^2}{2} x_j^2 + F_j(t)x_j \quad (11)$$

Second quantization leads to

$$H = \hbar\Omega_x \left(a^\dagger a + \frac{1}{2} \right) + F(t) \sqrt{\frac{\hbar}{2m\Omega_x}} (a + a^\dagger) . \quad (12)$$

The time evolution of this Hamiltonian can be solved following [19]. If the initial state is the vacuum state, the solution is a coherent state $|\alpha(t)\rangle = U(t)e^{-\frac{1}{2}|\alpha|^2} \sum_{n=0}^{\infty} \frac{\alpha^n}{\sqrt{n!}} |n\rangle$ with $U(t)$ global phase and parameter $\alpha(t)$

$$\alpha(t) = -i \frac{1}{\sqrt{2\hbar m \Omega}} \int_0^t dt' e^{i\Omega_x(t-t')} F(t') . \quad (13)$$

We assume the local force to be of the form $F_j(t) = A \cos(\omega_{dr}t + \phi_j)$ with A Amplitude, ω_{dr} the driving frequency and ϕ_j a local phase. For constant Amplitude A , the closer ω_{dr} to the eigen frequency of the harmonic oscillator, the larger α .

The driving energy is equal for $\phi = 0$ and $\phi = \pi$ and given as

$$\begin{aligned} F(t)\langle x \rangle &= F(t) \sqrt{\frac{\hbar}{2m\Omega_x}} 2\text{Re}(\alpha) \\ &= \frac{1}{m\Omega_x} \frac{A^2}{\Omega_x^2 - \omega_{dr}^2} \cos(\omega_{dr}t) \text{osc}(t) \end{aligned} \quad (14)$$

$$\text{osc}(t) = \Omega_x (\cos(\omega_{dr}t) - \cos(\Omega_x t)) . \quad (15)$$

This term both takes positive and negative values. For our special choice of driving the time average is $\lim_{T \rightarrow \infty} \frac{1}{T} \int_0^T \cos(\omega_{dr}t) \text{osc}(t) dt = \frac{\Omega_x}{2}$.

Due to the driving the system heats up, which is shown in an increase of mean excitation $\langle n \rangle$. The time average is given by

$$\overline{\langle n \rangle} = \overline{|\alpha(t)|^2} = \frac{A^2}{2\hbar m \Omega_x} \frac{(3\Omega_x^2 + \omega_{dr}^2)}{2(\Omega_x^2 - \omega_{dr}^2)^2} . \quad (16)$$

For the dipole energy we set $\phi_j = 0$ and $\phi_{j+1} = \pi$. By this choice of phases we have $\alpha_j = -\alpha_{j+1}$. This ensures that the two neighbouring dipoles are perfectly anti-correlated and the energy is

$$\begin{aligned} E_{dip-dip} &= \frac{Q^2}{4\pi\epsilon_0 r^3} \langle x_j \rangle \langle x_{j+1} \rangle \\ &= \frac{Q^2}{4\pi\epsilon_0 r^3} \frac{\hbar}{2m\Omega_x} 2\text{Re}(\alpha_j) 2\text{Re}(\alpha_{j+1}) \\ &= -\frac{Q^2}{4\pi\epsilon_0 r^3} \frac{1}{m^2\Omega_x^2} \left(\frac{A}{\Omega_x^2 - \omega_{dr}^2} \text{osc}(t) \right)^2 . \end{aligned} \quad (17)$$

This term can always be chosen to be negative, and oscillates between its extreme values $E_{min} \leq E_{dip-dip} \leq 0$.

Careful comparison of eq. 14, 16 and 17 shows that the induced heating due to driving is, except for very small distances, larger than the dipole-dipole energy reduction. This means that the non-equilibrium states considered here are not able to reduce the systems energy.

Discussion.— The system under study has continuous interaction between neighbouring sites. Therefore one might say the existence of entanglement is a triviality.

This is not the case for several reasons. Many systems are separable despite having continuous interaction. In our case, for long distances $r > 10\text{\AA}$ the system becomes almost separable. Also, the amount of entanglement, here measured by the negativity, could be vanishing small. If the interaction is reduced by setting $\epsilon = 0.01$, the system stays entangled, but with a vanishing amount of entanglement and the energy increases. Therefore, a high value of negativity goes along with small energy in this system.

This can be explained as follows. The coupling creates phonon modes, in which the movement of individual sites becomes correlated. The entanglement between sites allows these correlations to be in superposition states. Each site simultaneously oscillates in opposite directions. Because of the superposition states the oscillation of sites are correlated without net movement. Any classical correlation in oscillation will need to go along with net movement. This causes the system to heat up and is thus energetically less favourable than the quantum correlations.

Outlook. Our work, although it employs the simplest model possible, has important consequences. Firstly, it shows another counterexample to the believe that living systems are too hot and wet to sustain coherence and entanglement. The DNA base pairs are spatially separated and therefore form well defined subsystems. Due to the large trapping frequencies the system's state is well approximated by the ground state, which contains entanglement. Secondly, it shows why certain numerical procedures like *self-consistent charges density-fitting tight binding (SCC-DFTB)*, which does not cover dispersion energies, do not correctly describe the system's energy. Any local approach must fail if the system inhibits large amounts of entanglement. Quantum information has developed numerical tools like the matrix product states [20], which might improve the numerical work in quantum chemistry. Finally, it opens the field of discussion for possible consequences for the information content of DNA. What is the influence of entanglement for the readout of DNA? Is there any way to harness this entanglement?

Acknowledgments: E.R. is supported by the National Research Foundation and Ministry of Education, in Singapore. J.A. is supported by the EPSRC's QIPIRC programme. V.V. acknowledges financial support from the Engineering and Physical Sciences Research Council, the Royal Society and the Wolfson Trust in UK as well as the National Research Foundation and Ministry of Education, in Singapore.

- of dispersion energy. *J. Am. Chem. Soc.* **130** (47): 16055-16059, (2008).
- [2] G. S. Engel et al.: *Evidence for wavelike energy transfer through quantum coherence in photosynthetic systems*, *Nature* **446**, 782-786 (2007).
- [3] M. Mohseni, P. Rebentrost, S. Lloyd, A. Aspuru-Guzik: *Environment-assisted quantum walks in photosynthetic energy transfer*, *J. Chem. Phys.* **129**, 174106, (2008).
- [4] M.B. Plenio, S.F. Huelga: *Dephasing assisted transport: Quantum networks and biomolecules*, *New. J. Phys.* **10**, 113019 (2008).
- [5] F. Caruso, A.W. Chin, A. Datta, S.F. Huelga, M.B. Plenio, *J. Chem. Phys.* **131**, 105106 (2009).
- [6] J.-M. Cai, G. G. Guerreschi, H. J. Briegel: *Quantum control and entanglement in a chemical compass*, *Phys. Rev. Lett* **104**, 220502 (2010).
- [7] E. Gauger, E. Rieper, J.J.L. Morton, S.C. Benjamin, V. Vedral: *Quantum coherence and entanglement in the avian compass*, arXiv:0906.3725, (2009).
- [8] J.-M. Cai, S. Popescu, H. J. Briegel: *Dynamical entanglement in oscillating molecules*, arXiv:0809.4906, (2008).
- [9] H. J. Briegel, S. Popescu: *Intra-molecular refrigeration in enzymes*, arXiv:0912.2365, (2009).
- [10] J. Černý, M. Kabeláč, P. Hobza: *Loss of Dispersion Energy Changes the Stability and Folding/Unfolding Equilibrium of the Trp-Cage Protein*. *J. Phys. Chem. B* **113** (16): 5657-5660, (2009).
- [11] R. Luo, H. S. R. Gilson, M. J. Potter, M. K. Gilson: *The Physical Basis of Nucleic Acid Base Stacking in Water* *Biophys. J.* , **80**, 140-148, (2001).
- [12] A. Cohen , S. Mukamel: *Resonant enhancement and dissipation in nonequilibrium van der Waals forces*, *Phys. Rev. Lett.* **91**, (23), 233202 ,(2003).
- [13] E. Rieper , J. Anders, V. Vedral: *Entanglement at the quantum phase transition in a harmonic lattice*, *New J. Phys.* **12** 025017, (2010).
- [14] J. Anders: *Thermal state entanglement in harmonic lattices*. *Phys. Rev. A* **77** 062102 (2008).
- [15] G. Adesso , A. Serafini, F. Illuminati: *Extremal entanglement and mixedness in continuous variable systems*. *Phys. Rev. A* **70**, 022318 (2004).
- [16] Thanks to H. J. Briegel for pointing this out.
- [17] G.C. Maitland, M. Rigby, E. Brian Smith, W.A. Wakeham *Intermolecular forces* Clarendon Press, Oxford, (1981).
- [18] H. Barsch, D.R. Garmer, P.G. Jasien, M. Krauss, W.J. Stevens: *Electrical properties fo nucleic acid bases*, *Chem. Phys. Lett.*, **163**,6,514-522, (1989).
- [19] C. Gardiner and P. Zoller, *Quantum Noise* Springer-Verlag
- [20] J. Eisert, M. Cramer, M.B. Plenio: *Area laws for the entanglement entropy - a review*, arXiv:0808.3773, (2008).
- [21] Here entanglement describes non-local correlations, not inter-linking between polymers.

[1] J. Černý, M. Kabeláč, P. Hobza: *Double-helical ladder structural transition in the B-DNA is induced by a loss*